Use of the Thermodynamic Solution Properties of Xenon in *n*-Alkanes for the Examination of Models for the Cavity Formation Process

Jung Hag Park*, James E. Brady† and Peter W. Carr‡

Department of Chemistry, Yeungnam University, Gyongsan 713-749
†Department of Chemistry, University of Pittsburg, Pittsburg, PA 15260 U.S.A.
‡Department of Chemistry, University of Minnesota 207 Pleasant Street S.E. Minneapolis, MN 55455 U.S.A. *Received March 13, 1989*

The interaction energies of Xenon in n-alkanes were estimated by using three models for the cavity formation process, Hildebrand's regular solution theory, Pierotti's scaled particle theory and Sinanoglu-Reiss-Moura-Ramos' solvophobic theory in an attempt to examine the validity of three models. It appears that Pierotti's implementation of scaled particle theory yields a reasonable estimate of cavity formation energy over a considerable range in solvent size provided that the solute is spherical enough as are the inert gases.

Introduction

Recently Pollack *et al.*[1,2] reported measurements of the Ostwald solubility of Xenon in the *n*-alkanes and on the various thermodynamic functions for the process indicated below:

$$Xe(\text{gas, 1 atm}) \rightleftharpoons Xe(\text{solution, unit mole fraction}) \quad (1)$$

Equation 1 describes the solution process in which the solute in the gas phase at a given temperature and 1 atm pressure is transferred to solution in the liquid phase at the same temperature and hypothetical solute mole fraction of unity. The reproducibility was such as to allow calculation of the entropy and enthalpy of transfer from the temperature derivative of the free energy. As shown in Figure 1 all the principal transfer thermodynamic functions for xenon ($\Delta\mu°$, $\Delta S°$, and $\Delta H°$) vary monotonically with the carbon number of an *n*-alkane solvent. In contrast literature data[3] on the enthalpy and entropy of solution of helium, neon, argon and krypton show a great deal of scatter when plotted vs. the solvent carbon number (see Table 1, note the large uncertainties in the mean residual sum of squares and the large standard deviations in the slopes and intercepts for all solutes except Xenon).

A systematic relationship between the slope and the intercept of plots of $\Delta\mu°$ versus carbon number as the gas is varied from helium to Xenon is also indicated in Table 1. Although a plot (not shown) of the intercept versus the slope for the regression of the free energy against carbon number for each gas is quite linear (correlation coefficient = 0.998, average residual = 0.9), a similar analysis of the enthalpy shows a weak correlation between the slopes and intercepts (correlation coefficient = 0.78, average residual = 27).

These observations suggest that only the Xenon data of references 1 and 2, which was obtained by a vary precise radiochemical methodology, are suitable for assessing the accuracy of various models of estimating the free energy, enthalpy and entropy of transfer. The free energy data for the other gases, which were obtained by classical procedures, are not sufficiently precise to withstand the numerical differentiation with respect to temperature involved in the calculation of the enthalpy and entropy. Thus, our primary focus will be on the thermodynamic data for Xenon. Data for the other gases are available in only 7 *n*-alkanes[3], whereas that for Xenon is avilable for 12 *n*-alkanes (pentane to hexadecane).

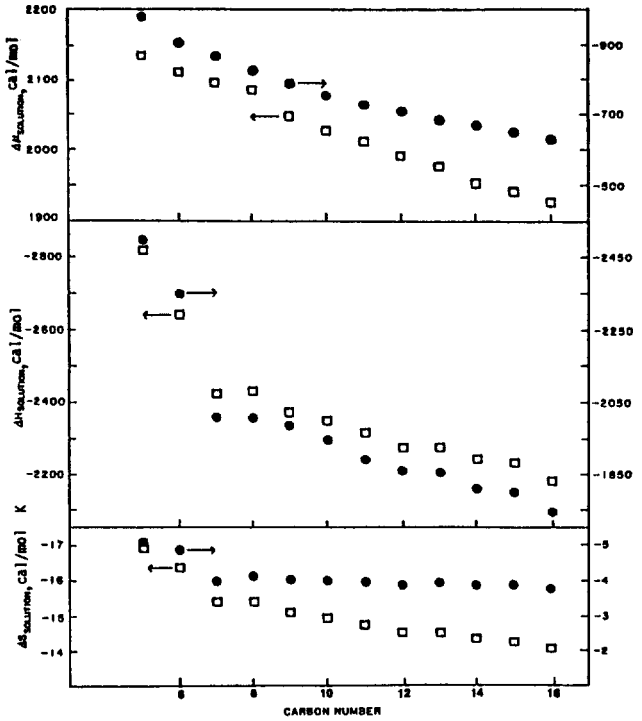

Figure 1. Plot of free energy, enthalpy and entropy of transfer for Xenon versus solvent homolog number: (a) mole fraction scale (□), (b) molar concentration scale (●).

A vexing problem that must be faced in interpreting thermodynamic results of the type described above is the choice of appropriate concentration scale. This choice is by no means trivial if one intends to apply the results in an extrathermodynamic analysis of the system. Ironically this issue is complicated to such an extent even in such a seemingly well

Table 1. Free Energy and Enthalpy of Transfer for Rare Gases to n-Alkanes

	$\Delta\mu°$[a]				$\Delta H°$[b]			
Gas	Intercept[c]	Slope[d]	r[e]	sd[f]	Intercept[g]	Slope[g]	r[g]	sd[g]
He[h]	4841 ± 20	10.9 ± 2	0.918	14.5	2365[j] ± 135	−60 ± 33	−0.63	115
Ne[h]	4631 ± 30	9.5 ± 3	0.809	21.4	1344 ± 204	15 ± 21	0.309	144
Ar[h]	3589 ± 15	−4.7 ± 1	−0.808	10.5	−514 ± 263	21 ± 27	0.326	186
Kr[h]	3009 ± 15	−9.8 ± 1	−0.947	10.3	−1204 ± 157	3 ± 16	0.094	111
Xe[i]	2223 ± 4	−19.4 ± 0.4	−0.999	2.9	−2761 ± 80	40 ± 8	0.908	58

[a] Free energy (mole fraction) in cal/mole at 25 °C. [b] Enthalpy of transfer (mole fraction) in cal/mole at 25 °C. [c] From intercept of plot of $\Delta\mu°$ *vs.* solvent homolog number. [d] From slope of plot of $\Delta\mu°$ *vs.* solvent homolog number. [e] Correlation coefficient. [f] Root mean square deviation. [g] Same as c-f except $\Delta H°$ is correlated. [h] Data from reference 3. [i] Data from reference 1 and 2. [j] Data point for nonane is deleted.

defined series as the *n*-alkanes that trends can be reversed simply by an alternate choice of concentration scale. One the other hand there are many non-thermodynamic probes of the solution process which do not depend upon the choice of a concentration scale (*e.g.* solvatochromism), in which solute-solvent energetics are directly probed. Two of us has recently examined solute-solvent energetics in the *n*-alkanes via solvatochromism[4]. The molecular interpretation of these results are at variance with previous studies of Xenon solubility[1-3]. Yet for these and other simple systems in which the interactions are exclusively dispersive[5-7], one expects optimal concordance between these disparate methodologies. In this regard Ben-Naim has persuasively argued[8,9] that the molecular interpretation of solution thermodynamics is greatly complicated by the concentration scale used to establish the reference state. In our view he has decisively argued in favor of the molar (mol/liter) and against the mole fraction concentration scale. We hope to adequately address this issue herein.

It is widely accepted that the overall solution process may be envisioned as taking place in two hypothetical steps[12,13]. First a cavity or hole of the correct shape and size to accommodate the solute is formed in the solvent, and second the cavity is filled with the solute and the solute is allowed to interact with the surrounding solvent environment. The cavity formation process is always endothermic (unfavorable) whereas the interaction process is always exothermic (favorable). Thus the free energy associated with solution can be described as the following:

$$\Delta\mu^*_{soln} = \Delta\mu_{cav} + \Delta\mu_{int} \quad (2)$$

In this regard, the examination of thermodynamic quantities for the overall solution process without separating it into two parts (the cavity formation and interaction processes) may not provide a clear understanding of the interactions involved. In this work we attempted to estimate the interaction energy terms using three cavity models[14-21] and examined the variation of the interaction energies of Xenon in the homologous series of *n*-alkanes. Provided that the estimated cavity terms are accurate, one can expect that the interaction terms will provide a clearer insight into the forces between Xenon and *n*-alkanes.

The Thermodynamic Quantities Associated with the Solution of Xenon in *n*-Alkanes. Because the Ostwald solubility (L) was the measured variable in references 1 and 2, a direct calculation of the molar concentration scale-based free energy, entropy and enthalpy of transfer of Xenon is possible without recourse to knowledge of the solvent density and its temperature dependence. Assuming a perfect gas, it is easily shown that:

$$\Delta\mu^* = -RT\ln L \quad (3)$$

where $\Delta\mu^*$ denotes the transfer free energy using the concentration units of moles per liter in both the gas and liquid phases. Thus, it is possible to obtain ΔS^* and ΔH^* from the slope and intercept of a plot of −RTlnL versus temperature assuming[2,9] that for each alkane ΔH^* and ΔS^* are constant over the temperature interval of the data:

$$-RT\ln L = \Delta H^* - T\Delta S^* \quad (4)$$

These results are summarized in Table 2 and Figure 1.

Table 2. Thermodynamic Functions for the Transfer of Xenon from the Gas Phase to the Solvent[a]

Solvent	Molar Volume[b]	$\Delta\mu^*$		ΔH^*		ΔS^*	
		soln[c]	int[d]	soln	int	soln	int
Pantane	116.12	−988	−4160	−2500	−5823	−5.07	−5.56
Hexane	131.62	−906	−4405	−2347	−5958	−4.84	−5.20
Heptane	147.46	−863	−4652	−2050	−5884	−3.98	−4.13
Octane	163.54	−822	−4845	−2049	−6074	−4.11	−4.12
Nonane	179.70	−789	−5103	−1984	−6313	−4.01	−4.06
Decane	195.94	−759	−5163	−1947	−6287	−3.99	−3.78
Undecane	212.0	−726	−5290	−1896	−6383	−3.93	−3.68
Dodecane	228.6	−706	−5412	−1859	−6480	−3.87	−3.59
Tridecane	244.7	−679	−5500	−1853	−6577	−3.94	−3.62
Tetradecane	261.31	−665	−5605	−1809	−6677	−3.84	−3.57
Pentadecane	277.5	−643	−5690	−1799	−6783	−3.88	−3.67
Hexadecane	293.4	−625	−5774	−1742	−6834	−3.75	−3.57

[a] At 25 °C based on molar concentration scale. Free energies and enthalpies in cal/mole; entropies in cal/mole °K. [b] From references 32 and 37. [c] Free energy of solution computed by Eq. (3) using data from references 1 and 2. [d] Computed interaction term by Eq. (2) based on measured free energy of solution and cavity term based on scaled particle theory.

Estimation of the Interaction Energies of Xenon with *n*-Alkanes by the Use of Cavity Models. Inspection of Table 2 indicates that the solution process ($\Delta\mu^*$) becomes less favorable as the alkane homolog number increases. This is quite the opposite of the trend that would be expected based solely on an anticipated increase in the strength of the solute-solvent interactions. Various independent measures of solvent strength (see Table 3) including solvent polarizabili-

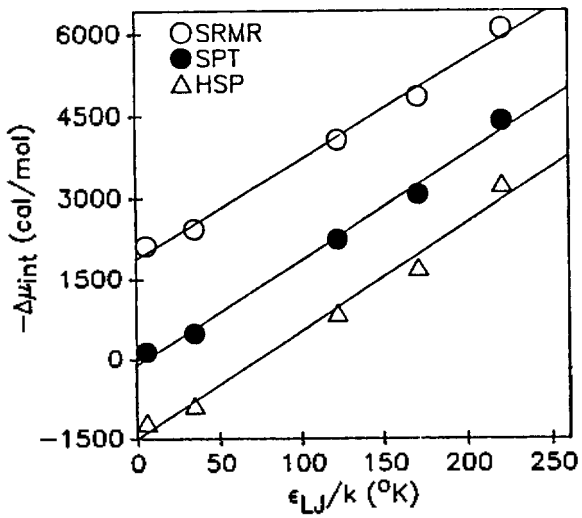

Figure 2. Plot of free energy of interaction of variation of various solutes in hexane versus solute ϵ_{LJ}: (a) Based on solubility parameter cavity energy (△), (b) Based on solvophobic cavity energy (○), (c) Based on scaled particle theory cavity energy (●).

Table 3. Physical Properties of the Alkanes (25 °C)

Solvent	$L(n^2)^a$	π^{*b}	δ^c	γ^d	α_p^e	y^f_{Pierotti}	y^g_{Bondi}
Pentane	0.2178	-0.087	7.03	15.49	1.555	0.445	0.500
Hexane	0.2274	-0.04	7.27	17.86	1.406	0.483	0.518
Heptane	0.2344	-0.033	7.43	19.65	1.281	0.514	0.532
Octane	0.2398	0.01	7.55	21.14	1.191	0.540	0.542
Nonane	0.2441	0.02	7.65	22.38	1.117	0.565	0.551
Decane	0.2476	0.03	7.73	23.37	1.060	0.579	0.557
Undecane	0.25041	0.04	7.79	24.21	1.013	0.594	0.562
Dodecane	0.25279	0.045	7.84	24.91	0.973	0.608	0.567
Tridecane	0.25485	0.056	7.89	25.55	0.940	0.620	0.571
Tetradecane	0.25663	0.066	7.92	26.13	0.913	0.631	0.574
Pentadecane	0.25805	0.07	7.97	26.64	0.889	0.641	0.577
Hexadecane	0.25962	0.08	7.99	27.05	0.866	0.650	0.579

[a] Refractive indices from reference 32. [b] From reference 4. [c] Solubility parameter (cal/cc)$^{1/2}$ from references 33-34. [d] Surface tension (dyne/cm) from reference 35. [e] Thermal expansion coefficient ($\times 10^3$/°K) from reference 37. [f] Packing fraction computed according to Pierotti's method (equation 12). [g] Packing fraction as ratio of Bondi volume to molar volume.

ty, solubility parameter, and the Kamlet-Taft empirical π^* scale indicate that the hexadecane-Xenon interaction ought to be stronger than the pentane-Xenon interaction.

To resolve this apparent discrepancy one should envision the overall solution process as the sum of two almost independent events. First, a cavity or hole of the proper shape and size to accommodate the solute is formed in the solvent; second the cavity is charged with the interaction properties characteristic of the solute (polarizability, dipole moment, *etc.*). Of course these two processes are not perfectly independent; the solute may change the local solvent structure. However, the free energy of solvent reorganization is expected to be negligible for the systems studied here[10,11]. Many phenomenologically distinct models of solution including regular solution theory[12,13], Sinanoglu's solvophobic theory[14-17], and scaled particle theory[18-21] share this two-stage view of the overall solution process.

Table 4. Interaction Energies of Rare Gases with *n*-Hexane at 25 °C

Solute	a_2^a	V^b	ϵ^c	$\Delta\mu_{int,H}{}^d$	$\Delta\mu_{int,srmr}{}^e$	$\Delta\mu_{int,spt}{}^f$
Helium	2.63	11.5	6.03	1190	-2124	-143
Neon	2.78	13.5	34.9	870	-2432	-488
Argon	3.40	24.8	122	-859	-4061	-2243
Krypton	3.60	29.4	171	-1709	-4843	-3065
Xenon	4.10	43.5	221	-3243	-6092	-4405

[a] Hard sphere diameter (Å). [b] Molar volume (cc/mol) estimated as twice the hard core volume. [c] Lennard-Jones interaction energy(°K). [d] Interaction energy based on regular solution theory estimate of the cavity formation energy (cal/mol). [e] Interaction energy based on solvophobic-surface tension model of the cavity formation energy (cal/mol). [f] Interaction energy based on the scaled particle theory model of the cavity formation energy (cal/mol).

The energy expended in forming a cavity was estimated using the following equations:

$$\mu^*_{\text{cav,H}} = V_2\delta_1^2 \tag{5}$$

$$\mu^*_{\text{cav, SRMR}} = \Delta H_{\text{vap},1} + 9.761\,(V_2^{2/3} - V_1^{2/3})\,\gamma_1 \tag{6}$$

$$\mu^*_{\text{cav, SPT}} = K_0 + K_1 a_{12} + K_2 a_{12}^2 + K_3 a_{12}^3 \tag{7}$$

where the subscript 1 and 2 denote the solvent and solute; H, SRMR and SPT designate the Hildebrand solubility parameter, Sinanoglu's solvophobic (as modified by Reisse and Moura-Ramos) and the scaled particle models, respectively. V, δ, and γ respresent the solute or solvent molar volume, the solvent solubility parameter, and the solvent surface tension. According to Pierotti, a_{12} is the radius of a sphere that excludes the centers of both the solvent and solute molecules. The coefficients K_0-K_3 are given below:

$$K_0 = RT\{-\ln(1-y) + (9/2)z^2\} - \pi P a_1^3/6 \tag{8}$$

$$K_1 = (-RT/a_1)\,(6z + 18z^2) + \pi P a_1^2 \tag{9}$$

$$K_2 = (RT/a_1^2)\,(12z + 18z^2) - 2\pi P a_1 \tag{10}$$

$$K_3 = (4/3)\,\pi P \tag{11}$$

$$z = y/(1-y) \tag{12}$$

where $y = \pi a_1^3 \rho_1/6$, ρ_1 is the number density of the solvent, a_1 is the equivalent hard sphere diameter of the solvent, P is the pressure, R is th gas constant, and T is temperature. The term y represents the solvent packing fraction.

Pierotti advises that scaled particle theory be used in a semiempirical fashion so as to preserve as much information on the solvent as possible. Consequently we have adopted his procedure and used the experimental density and pressure rather than those computed from the theoretical equation of state. Furthermore, Pierotti obtained the equivalent hard sphere diameter of the solvent from the experimental heat of vaporization (ΔH_{vap}) and thermal expansion coefficient (α_p):

$$\Delta H_{\text{vap}} = RT + \alpha_p RT^2\,[(1+2y)^2/(1-y)^2] \tag{13}$$

The interaction energy was obtained from the free energy of solution and the estimated cavity formation energy as follows:

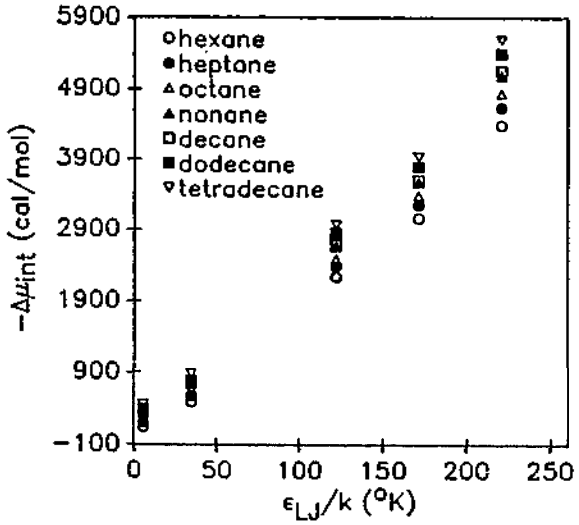

Figure 3. Plot of free energy of interaction based on scaled particle theory versus ϵ_{LJ}.

$$\Delta\mu_{int} = \Delta\mu^{*}_{soln} - \Delta\mu_{cav} \quad (14)$$

The results of the computation for all of the rare gases with *n*-hexane as the solvent are given in Table 4. Values of the free energy of solution for He through Kr (on the molar concentration scale) were obtained from the data in references 1-3 and the solvent molar volume as follows:

$$\Delta\mu^{*} = \Delta\mu^{\circ} - RT\ln(RT/pV_1) \quad (15)$$

In order to compute the cavity term, it is necessary to estimate the molar volume of the solute (see eq. 5). We arbitrarily chose a value of twice the hard core volume in all cases. Table 4 shows that with *n*-hexane as the solvent, the solubility parameter model greatly underestimates the cavity formation energy leading to impossible positive interaction energies for helium and neon. This model also yields the physically counter-intuitive result that the interaction energy of the gases except Xenon becomes less favorable as the solvent homolog number increases. We conclude that solubility parameter theory does not generate an accurate estimate of the cavity formation free energy unless an excessively large value is taken for the molar volume of the solute gas.

The Reisse-Moura-Ramos modification of Sinanoglu's solvophobic model (SRMR) produces the most negative interaction energy of the three approaches (see Table 4). The energy is negative for all solute-solvent combinations and the direction of the trend with both the solute and solvent is as expected. We note that the change in $\Delta\mu_{int}$ from helium to Xenon in hexane by all three methods are rather similar (-4000 ± 200 cal/mole). However, we believe that SRMR overestimates the cavity formation energy. Inspection of the results in Table 4 clearly indicate that the SRMR based interaction energies are too negative. With hexane as the solvent, a plot of this energy versus the solute gas Lennard-Jones energy (ϵ_{LJ}) parameter has an very large negative intercept (see Figure 2). Thus while the solubility parameter approach underestimates the cavity formation energy, SRMR overestimates the cavity formation energy if the same solute molar volume is used in each calculation.

In contrast, the results based on the use of scaled particle theory appear to be more reasonable. Figure 3 indicates that

Table 5. Correlation of Free Energy of Interaction Based on Scaled Particle Theory with ϵ_{LJ}

Solvent	Intercept[a]	Slope[b]	r^c	sd[d]
Hexane	-111(133)	19.6(1.0)	0.996	175
Heptane	-56(140)	20.5(1.0)	0.996	185
Octane	-9(194)	21.0(1.1)	0.996	194
Nonane	60(160)	21.8(1.2)	0.995	210
Decane	57(161)	22.1(1.2)	0.995	210
Dodecane	80(171)	23.1(1.3)	0.996	225
Tetradecane	141(173)	23.7(1.3)	0.996	228

[a]Intercept in plot of $\Delta\mu^{*}_{int,spt}$ versus ϵ_{LJ}. [b]Slope of plot of $\Delta\mu^{*}_{int,spt}$ versus ϵ_{LJ}. [c]Correlation coefficient. [d]Root mean square deviation. [e]Standard deviations are indicated in parentheses.

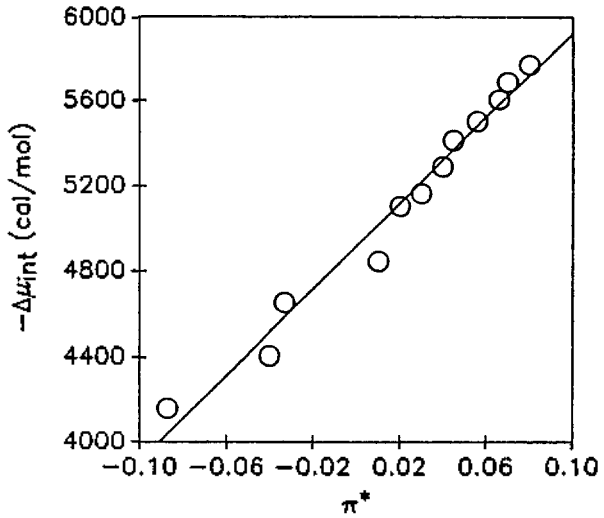

Figure 4. Plot of free energy of interaction of Xenon versus Kamlet-Taft dipolarity-polarizability of the solvent.

the interaction energy obtained by SPT (see Table 2) is a smooth function of ϵ_{LJ} and most importantly the intercept at zero solute energy in all solvents is quite small. In principle the interaction should be linear with $(\epsilon_{LJ})^{1/2}$ [18]. This may account for the slight upward curvature in Figure 2 and 3. The computed free energy of interaction for each solute was regressed against the solute ϵ_{LJ} while the solvent was held constant. The results are presented in Table 5. In all cases the intercept at zero ϵ_{LJ} is statistically zero, the regression coefficient exceeded 0.995 and the average deviation of the fit was, at most, only third of RT. Thus, in all solvents studied, Pierotti's approach to SPT produces chemically reasonable estimates of the cavity formation energy of a non-interacting particle ($\epsilon_{LJ} = 0$). Further, there is little change in the slope of this plot as the solvent is varied. In view of the similarity of the methyl and methylene groups and the small size of the test solutes relative to all of the solvents this agreement is expected.

Discussion

The variation of the interaction energy with solvent is shown in Figure 4. as a plot *vs.* the empirical π^{*} measure of solvent strength. Recent work[4] has shown that for π^{*} for the *n*-alkanes as solvent is linearly correlated with both the

Table 6. Correlation of Free Energy[a] and Enthalpy[a] of Interaction of Xenon with Measures of Solvent Strength

Property	n	Intercept	Slope[b]	r	sd^c_{avc}
π^{*d}	11	-4.81 ± 0.02	-11.1 ± 0.4	0.994	49
$L(n^2)^d$	11	5.11 ± 0.4	-41.5 ± 1.5	0.994	52
δ^d	11	9.11 ± 0.03	-18.46 ± 0.004	0.999	3
π^{*e}	11	-6.47 ± 0.03	-9.1 ± 0.6	0.979	77
$L(n^2)^e$	11	1.61 ± 0.6	-33.9 ± 2.6	0.973	87
δ^e	11	4.86 ± 0.95	-1.51 ± 0.1	0.971	91

[a]Kcal/mol. [b]Kcal/mol. [c]cal/mol. [d]Free energy of interaction. [e]Enthalpy of interaction.

Table 7. Effect of Solvent on the Interaction Energy of Xenon at 25 °C[a]

Solvent	$\Delta\mu^*_{int,spl}/L(n^2)$	$\Delta H^*_{int,spl}/L(n^2)$
Pentane	-19.1	-26.7
Heptane	-19.4	-26.2
Octane	-20.2	-25.3
Nonane	-20.9	-25.8
Decane	-20.8	-25.4
Undecane	-21.1	-25.5
Dodecane	-21.4	-25.6
Tridecane	-21.6	-25.8
Tetradecane	-21.8	-25.9
Pentadecane	-22.0	-26.3
Hexadecane	-22.2	-26.3
Average	-20.8	-25.8

[a]All results in Kcal/mol.

solubility parameter (δ) and Lorentz function of refractive index [$L(n^2) = (n^2-1)/(n^2+2)$]. The Kirkwood-Muller (*K-M*) equation shows that the interaction term is related, although not linearly, to the solvent molecular polarizability[16]. Although Abraham *et al.*[16] indicate that the *K-M* approach is quantitatively incorrect for alkanes and other complex fluids, the existence of good correlations between π^* and δ with $L(n^2)$ suggests that this regression should also be examined. Results of the linear regression analysis are shown in Table 6. In all cases a statistically significant (repulsive) intercept is obtained which does not correspond to the expected value for zero solvent strength (or polarizability). That is, when either $L(n^2)$ or δ are equal to zero, we anticipate that the interaction will be nil. Similarly, at the gas phase value of π^* (-1.06 ± 0.10[22]) we expect the interaction to become zero. This is not observed. However, in this case the extrapolation is large relative to the range of the data. Thus, a small *determinate* error in the slope or curvature in the relationship will be greatly exaggerated and will lead to spurious results. Non-linearity in the relationship can be more clearly defined by examining the ratio of these two quantities. The results are shown in Table 7. A monotonic trend in the ratio is evident although it is only 14% from smallest to largest. Despite the small size of this discrepancy we believe that it is real and it is likely the result of a problem with the input data. In particular it can be shown that errors in the hard core diameter of the solute would have to be much too large to account for the problem: However the computed interaction energies and their dependence on the above mentioned solvent strength parameters are very sensitive to systematic trends in the packing fraction (y) as the solvent molar volume increases. When y was estimated as the ratio of the Bondi volume[23] to the solvent molar volume, the value of y increased monotonically with homolog number as did the value estimated via equation 13. In addition the net change in y was a good deal smaller and the slope of a plot of the interaction free energy of transfer for Xenon against any of the solvent parameters became slightly positive. The Stearn-Eyring equation for the hard core radius gives a constant value of y equal to $\pi/6$ for all solvents[24].

Wilhelm has pointed out the importance of using consistent estimates of the hard sphere diameter of the solute and solvent[25] to obtain meaningful free energies and entropies of cavity formation. In the present study the size of the solute is much better defined than is that of the solvent.

The results were also examined by estimating the enthalpy of cavity formation from scaled particle theory and computing the enthalpy of interaction from the measured heat of solution (see Table 7). Here the difference between the largest and smallest is only 7% and the trend in the ratio is not all monotonic.

The data can be examined in an entirely different fashion as follows: We assume that the free energy or enthalpy of interaction of Xenon with an *n*-alkane can be represented as the sum of appropriately weighted interaction of Xenon with each type of group (CH_2 and CH_3) in the solvent. This is similar to the approach used by Ben-Naim[9]. The number of interactions is assumed to be proportional to the volume fraction of that group, as defined by its hard core volume, relative to the total volume of solution. Because methyl and methylene groups are chemically similar and the sole type of interaction between Xenon and these groups is dispersive this would seem a reasonable assumption. Combining the interaction term and the group volume terms we may write:

$$\Delta\mu_{int} = \{\theta(CH_3)\, n(CH_3) + \theta(CH_2)\, n(CH_2)\}/V_1 \qquad (16)$$

where $\theta(CH_3)$ and $\theta(CH_2)$ denote the free energy of interaction of CH_3 and CH_2 group, $n(CH_3)$ and $n(CH_2)$ indicate the number of CH_3 and CH_2 groups in the alkane solvents, respectively. This suggests regressing the term $\Delta\mu_{int}\, V_1$ or $\Delta H_{int}\, V_1$ against the number of methylene groups in the alkane. The results are as follows:

$$\Delta\mu_{int}V_1/10000 = -13.55\,(\pm 0.7) - 11.07\,(\pm 0.07)\, n(CH_2)$$

$$n=12,\quad r=0.99978,\quad sd=0.9 \qquad (17)$$

$$\Delta H_{int}V_1/10000 = -27.58\,(\pm 1.6) - 12.21\,(\pm 0.17)\, n(CH_2)$$

$$n=12,\quad r=0.99898,\quad sd=2.1 \qquad (18)$$

Extrapolation to zero methylene groups leaves two methyl groups thus the negative intercept is entirely reasonable. Further we note that the slope of the two regressions are similar, as expected, although they are statistically different. The interaction parameter of Xenon with a methyl group relative to that with a methylene can be computed from the slope and intercept. The results are 0.61 and 1.12 with the free energy and enthalpy data, respectively. The interaction strength and polarizability of a methyl group is generally considered to be slightly greater than that of a methylene

group[26,27] thus the result from the enthalpy seems to be more reasonable.

While it is undoubtedly true that *n*-alkanes are not hard spheres and are more appropriately treated as hard convex bodies (for example by the equations developed in reference 38) Pierotti's semi-empirical method (eq. 13) likely compensate for solvent asphericity to a considerable extent. Indeed, the hard core diameter grows more rapidly with homolog number than does the same parameter based on estimates computed from the Bondi volume[23].

Conclusion

It has been shown in this work that the use of the interaction energies obtained by a cavity model and the examination of the variation of the interaction energies of Xe in homologous *n*-alkanes provide a better understanding of inert gas-organic solvent interactions than studying the overall solution properties associated with solution process[2,9].

It appears that Pierotti's implementation of scaled particle theory recovers a reasonable estimate of cavity formation energy over a considerable range in solvent size provided that the solute is spherical enough as are the inert gases. Several groups have questioned the validity of scaled particle theory when large solutes are examined[28,29]. In view of the renaissance of interest in the application of SPT to solutions of fixed gases in water[30,31] its present application in an unstructured solvent underscores the strength and weakness of the methodology.

Acknowledgement. We thank Prof. J. Reisse and Dr. J. J. Moura Ramos for their helpful comments on their method of calculating cavity terms.

References

1. G. L. Pollack, *J. Chem. Phys.*, **75**, 5876 (1981).
2. G. L. Pollack and J. F. Himm, *J. Chem. Phys.*, **76**, 3221 (1982).
3. E. Wilhelm and R. Battino, *Chem. Rev.*, **73**, 1 (1973).
4. J. E. Brady and P. W. Carr, *J. Phys. Chem.*, **89**, 1813 (1985).
5. K. L. Lewis, L. Q. Labo, and L. A. K. Snaveley, *J. Chem. Thermodyn.*, **10**, 351 (1978).
6. J. C. G. Calado and L. A. K. Snaveley, *Trans. Faraday Soc.*, **67**, 289 (1971).
7. W. H. Yunker and G. D. Halsey, *J. Phys. Chem.*, **64**, 484 (1960).
8. A. Ben-Naim, *J. Phys. Chem.*, **82**, 792 (1978).
9. A. Ben-Naim and Y. Marcus, *J. Chem. Phys.*, **80**, 4438 (1984).
10. R. Lumry and R. Rajender, *Biopolymers*, **9**, 1125 (1970).
11. A. Ben-Naim, *Biopolymers*, **14**, 1337 (1975).
12. J. H. Hildebrand, J. M. Prausnitz, and R. L. Scott, Regular and Related Solutions, Van Nostrand: New York; 1970.
13. K. Shinoda, Principles of Solution and Solubility, Marcel Dekker Inc.: New York; 1978.
14. O. Sinanoglu, in Molecular Associations in Biology, B. Pullman (Ed.), Academic Press: New York; p. 427, 1968.
15. T. Halicioglu and O. Sinanoglu, *Ann. N. Y. Acad. Sci.*, **158**, 308 (1969).
16. J. J. Moura-Ramos, J. Reisse and M. H. Abraham, *Can. J. Chem.*, **57**, 500 (1979).
17. J. J. Moura-Ramos, M.-L. Stier, and Reisse, *J. Chem. Phys. Lett.*, **42**, 373 (1976).
18. R. A. Pierotti, *J. Phys. Chem.*, **67**, 1840 (1963).
19. R. A. Pierotti, *Chem. Rev.*, **76**, 717 (1976).
20. R. A. Pierotti, *J. Phys. Chem.*, **69**, 281 (1965).
21. R. O. Neff and D. A. McQuarrie, *J. Phys. Chem.*, **77**, 413 (1973).
22. M. Essafar, J. L. Guiheneuf, and J. L. Abboud, *J. Am. Chem. Soc.*, **104**, 6786 (1982).
23. A. Bondi, *J. Phys. Chem.*, **68**, 441 (1964).
24. A. Stearn and H. Eyring, *J. Chem. Phys.*, **5**, 113 (1937).
25. E. Wilhelm, *Fluid Phase Equilibria*, **27**, 233 (1986).
26. J. H. Hildebrand, *Proc. Natl. Acad. Sci. (USA)*, **76**, 6040 (1979).
27. K. J. Miller and J. A. Savchik, *J. Am. Chem. Soc.*, **101**, 7206 (1979).
28. B. Lee, *J. Chem. Phys.*, **83**, 2421 (1985).
29. B. Lee, *J. Phys. Chem.*, **87**, 112 (1983).
30. B. Lee, *Biopolymers*, **24**, 813 (1985).
31. R. Fernandez-Prini, R. Crovetto, M. L. Japas, and D. Laria, *Acc. Chem. Res.*, **18**, 207 (1985).
32. J. A. Riddick, N. B. Bunger, Organic Solvents. Physical Properties and Methods of Purification, Wiley-Interscience: New York; 1970.
33. S. Wingefors and J. O. Liljenzen, *J. Chem. Technol. Biotechnol.*, **31**, 115 (1981).
34. S. Wingefors and J. O. Niljenzen. *J. Chem. Technol. Bioetchnol.*, **31**, 523 (1981).
35. J. J. Jasper, *J. Phys. Chem. Ref. Data*, **1**, 841 (1972).
36. B. J. Zwolinski, *et al.*, Selected Values of Properties of Hydrocarbons and Related Compounds, API Research Project #44: Texas A&M University; 1978.
37. W. A. Van Hook, *Fluid Phase Equilibria*, **22**, 55 (1985).
38. T. Boublik, *J. Chem. Phys.*, **63**, 4084 (1975).